Investigation of Hydrogen Peroxide Formation After Underwater Plasma Discharge

T. Nguyen, C. Rond, A. Vega, X. Duten, Sébastien Forget

Investigation of hydrogen peroxide formation after underwater plasma discharge

T.S. Nguyen[1], C. Rond[1], A. Vega[1], X. Duten[1] and S. Forget[2]

[1] LSPM—CNRS UPR 3407, Université Paris 13, Villetaneuse, 93430, France

[2] LPL- UMR 7538, Université Paris 13, Villetaneuse, 93430, France

E-mail: rond@lspm.cnrs.fr

ABSTRACT

This paper reports investigations on the formation of hydrogen peroxide resulting from micro-pulse plasma discharges obtained in pin-to-pin configuration underwater. In particular, this study reports the influence of the discharge regime (cathode regime with and without breakdown, and anode regime) as well as that of the discharge energy (from 10 to 45 mJ per pulse). It has been shown that the H_2O_2 production is higher for high energy and anode regime. In addition, the variation of the pulse width (from 50 to 500 µs) highlights the dependence of the chemical processes induced by the discharge according to the regime. Considering two different electrode materials (tungsten and platinum), we do not observe any significant influence of the electrode material on the H_2O_2 production, whereas the injected energy depends on the high voltage electrode material. Finally, the erosion of the electrodes have been studied using in-situ optical microscopy and SEM. It is shown that the erosion mechanisms strongly depend on materials, regimes and the polarity of the electrodes.

KEYWORDS: Underwater plasma, pulsed electrical discharge, pin-to-pin geometry, electrode erosion, hydrogen peroxide formation.

1. **Introduction**

The study of electrical discharges formed under water is of great interest because of their large applications in material, environmental and biomedical sciences [1-5]. Indeed a series of physical and chemical processes formed by discharges in the water lead to the production of various reactive chemical species such as radicals (OH, H, O), molecular species (H_2O_2, H_2, O_2, O_3) and solvated electron (e^-) [2, 5-8]. Their concentrations are obviously strongly dependent on the experimental conditions. In the frame of industrial applications, there is a need to determine these relationships in order to master and optimize the process. Most of the underwater discharges have been performed using pin-to-plate electrode configuration, of which the works of Locke and Lukes groups [6, 7, 9-17] are major contributions in valuable insights in chemical analysis. As an example, it has been shown that the early chemical activity is related to OH and H radicals formed by electron collisions with water molecules in the plasma channel [6]. It has been also demonstrated that the rate production of molecular hydrogen and hydrogen peroxide is 1:2 [7] and that the recombination of hydroxyl radicals is the major pathway to H_2O_2 formation[14, 15]. A special attention has been paid on the study of hydrogen peroxide production according to the experimental conditions such as the discharge treatment time [7, 9-13, 18, 19] the solution conductivity [6, 7, 11], the discharge power [6, 7, 10, 12], the gas flow [9, 19], the reactor configuration [12], the pH [19] and the electrode material [11, 13, 19, 20]. These discharges can produce about $k=5.10^{-7}$ M/s of H_2O_2 with high energy consumption (about 1 J/pulse). An exhaustive review discussing the methods to form hydrogen peroxide in electrical discharges with liquid water is available [16]. It reports that the energy yields are within the range from 0.5 to 1 $g.kWh^{-1}$ for a very wide range of types of discharge suggesting that a common mechanism drives the H_2O_2 formation.

In order to reduce this consumption, a needle-to-needle underwater discharge was used with low pulse energy (about 10 mJ) using reduced voltage (< 4 kV) but high frequency (10 kHz) and bipolar pulses [18]. The electrodes, made either in stainless steel or tungsten, are 1 mm diameter and the solution conductivity is high (from 500 to 1250 µS/cm). They have measured H_2O_2 concentration up to 5 mM independently of the type of plasma discharge (bridged or not). However, it is known that the

erosion of needle electrode involves the modification of the electrical field distribution since it is very sensitive to the electrode curvature radius. It is then possible to observe time evolution of the discharge characteristics, which is not suitable for industrial applications.

As a consequence, in parallel to the H_2O_2 production measurements, several studies focused on electrode erosion in underwater pulsed discharge [11, 13, 18, 20-22]. In particular these studies investigated the catalytic effect of W which leads to H_2O_2 decomposition [11, 13, 18, 23-27]. Possible mechanisms causing electrodes erosion by electrical discharge in water include melting, evaporation, electron/ion bombardment, sputtering, oxidation, cavitation…[21, 28]. As mentioned previously, most of the studies dealt with pin-to-plane configuration and they focused on the erosion of the HV-pin electrode [11, 13, 21] according to electrode material or solution conductivity. In particular, Lukes *et al* [11, 20] have reported that the anodic electrolysis is the significant form of erosion of the HV electrode [29] which can represent 40% of the total erosion process for tungsten or stainless steel electrodes [11, 20, 22]. In addition, thermal processes of erosion involving melting and condensation have been suggested [11, 20-22]. Potocký *et al* [18] have investigated the erosion of tungsten and stainless steel needle electrodes and the presented results suggest that the erosion mechanisms are similar on HV and GND for both materials and are also related to electrolysis and thermal processes. One mean of reducing the erosion issue is to decrease the diameter of the electrode enough that the discharge characteristics do not depend anymore on the shape of the tip, resulting in the pin-to-pin geometry that we used in the present work.

In this paper, we report the measurement of H_2O_2 production and electrodes erosion after underwater discharge using pin-to-pin configuration and low energy for different discharge regimes. Considering these experimental conditions, two different regimes have been identified (cathode and anode regimes) in which three different cases of discharge occur. A detailed description is given in [30]. As a summary, the cathode regime involve the case 1, in which a bush-like structure propagates from the cathode to the anode, a glow discharge appears on the cathode and no breakdown occurs between the two electrodes; and the case 2, where the bushy structure still appears at the cathode but the discharge spans the electrode gap causing the

breakdown. The anode regime corresponds to the case 3, where a filament structure appears and propagates from the anode to the cathode leading to several successive breakdowns.

In this work, a series of experiments were performed for different cases of discharge by changing the applied voltage, the pulse frequency and the pulse duration in order to determine the production of hydrogen peroxide. We also report the effect of different electrode materials (Tungsten and Platinum) on the production of hydrogen peroxide. The final section presents a study of the electrode erosion by the pulsed electrical discharge in water according to the material and the case of the discharge.

2. Experimental set-up

The scheme of the experimental set-up is presented in Fig.1. Pin electrodes of 100 µm diameter are covered by an insulating capillary tube. The length of both pin electrodes protruded from the capillary tube in water is about 400 µm (±100 µm). The distance between the two electrodes is set at 2 mm for all experiments. Most of the experiments are performed using tungsten electrodes, but use of platinum is also considered (see parts 3.5 & 4). The pin-to-pin geometry of electrodes has been used in two different reactors for two different kinds of experiments. Experiments investigating H_2O_2 concentration during the discharge are performed in a 200 mL cylinder glass reactor, whereas experiments dedicated to the variation of electrodes length involve a 150 mL rectangular reactor including two parallel silica windows for optical access. Changing the shape and the volume of the vessel does not involve significant variations on the final results on either H_2O_2 or electrodes measurements (lower than the estimated uncertainties).

The high voltage pulsed power supply consists of a low inductance capacitor (C = 1 nF) charged by a 30 kV DC high voltage supply passing through a 30 kΩ resistor which discharges through a fast high voltage solid-state switch (Behlke HTS 301-03-GSM). The positive high voltage pulse has a rising time equal to 30 ns and adjustable pulse duration from Δt = 50 µs to 1 ms. The pulse frequency is adjusted from f = 5 Hz to 100 Hz and the voltage range is between U = 4 kV and 11 kV. Discharge voltage and current waveforms are measured via a Tektronix high voltage probe connected to the high voltage electrode and a 10 Ω resistor connected with the

ground electrode respectively. Both signals are recorded by a digital oscilloscope (Lecroy HDO9104) every five minutes during the 30 min long experiment.

The conductivity of the solution is kept constant at σ=200 µS/cm for various experiments by using sodium chloride (NaCl). A magnetic stirring bar at the bottom of the reactor with speed of 200 rpm is used to homogenize the solution.

The concentration of hydrogen peroxide is determined by measuring the absorbance at 410 nm of the product of 2 mL sample with 1 mL of titanyl ions giving a yellow-colored complex [31]. These *ex-situ* measurements are performed in Avaspec-DHC2048XL spectrometer. Measurements are performed every 5 minutes during the 30 min long experiment. Uncertainty on H_2O_2 concentration is estimated to be lower than 2%. Both electrodes are imaged on a CCD Camera (IDS Imaging Development Systems) through a homemade microscope with a (×2)-magnification. A long working distance objective (Mitutoyo plan apochromatic, infinity corrected) was used to take into account the dimension of the reactor and coupled to a tube lens with a f=200 mm focal length. This optical system allowed in situ and real time measurement of the variation of the electrodes length during the plasma discharge (presented in Fig.1) with an accuracy of about 98%. Morphology and composition of the electrodes after the discharge are also studied ex-situ by using Scanning Electron Microscopy (SEM) and Energy-Dispersive X-ray spectroscopies (EDX) respectively.

For both, H_20_2 and electrode length measurements, a minimum of three measurements have been carried out for each experimental condition in order to ensure the reproducibility of the observed phenomena, and to provide reliable analysis of the results.

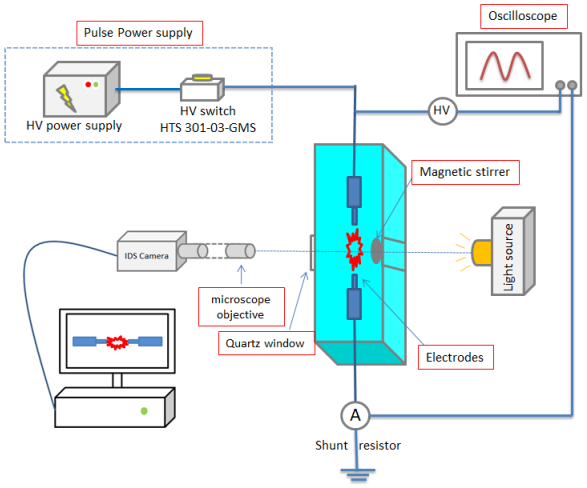

Fig. 1 Schematic diagram of the experiment set-up (150 mL rectangular reactor is shown).

3. H_2O_2 measurements

Basic experimental conditions involve tungsten wire for both electrodes and a pulse frequency fixed at 50 Hz (if no other specification).

3.1 Characteristics of the discharge

Fig.2(a) shows the typical voltage and current waveforms obtained for one pulse with different applied voltages (4, 6 and 9 kV). Detailed analysis of the waveforms can be obtained in [30]. The value of the applied voltage has been determined in order to obtain the three cases of discharge mentioned previously with f=50 Hz [30, 32]. Indeed, even if the occurrence of the different cases is random for given initial conditions, it is possible to identify a set of experimental conditions that makes a case dominant. Accordingly, case 1, case 2 and case 3 of the discharge correspond to applied voltages of 4 kV, 6 kV, and 9 kV respectively.

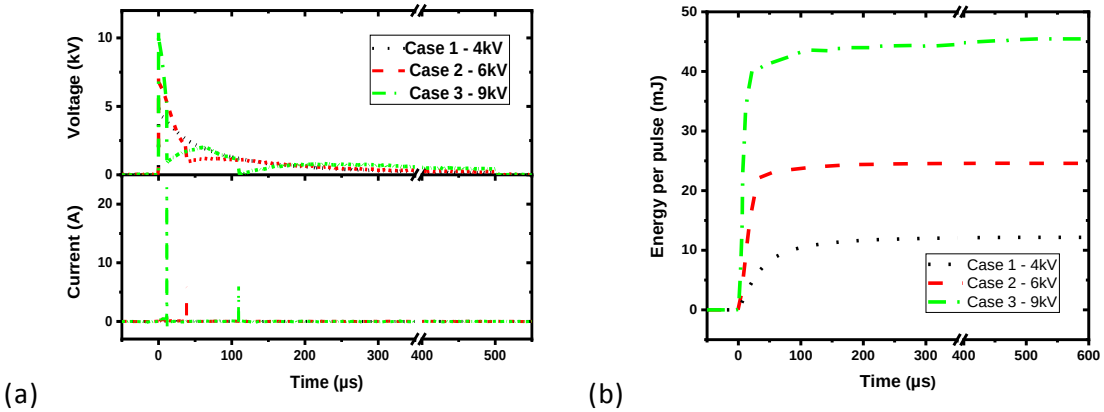

Fig.2 Typical electrical waveforms of pin-to-pin discharge generated in water: V = 200 mL, f = 50 Hz, Δt = 500 µs, 2 mm of gap, and σ = 200 µS/cm); (a) Voltage and Current signals and (b) Time evolution of the energy per pulse

In addition to identifying the case of the discharge, electrical signals are used to estimate the energy delivered to the discharge. The energy per pulse results from the time integration of the current and voltage product (Fig. 2(b)). We observe that most of the energy is deposited in the liquid during the first 50 µs of the discharge. Since the variation of the waveforms from pulse to pulse is lower than 10%, we determine the average energy per pulse by considering the average of all the waveforms measured (every 5 min) during the experiment. As an example for the experimental conditions reported in Fig.2, the average energy per pulse delivered for case 1 is about 12 mJ, for case 2 is 24 mJ and for case 3 is 45 mJ (reported on Fig.3(b)). We also determined the total energy of the process by integrating the average energy per pulse over the total duration of the experiment considering the frequency of the pulse generation. Considering the same example, we obtained a total energy equal to 1.1 kJ for case 1, 2.4 kJ for case 2 and 4.1 kJ for case 3.

3.2 Production of H_2O_2

The time evolution of H_2O_2 production was obtained by sampling 2 mL of the solution every 5 min (Fig.3(a)). After 30 min of discharge, the concentration of H_2O_2 remained very low in case 1 (< 0.1 mM); it reaches 0.3 mM in case 2; whereas the value is the highest one in case 3 with almost 0.8 mM. Moreover, the detection time of H_2O_2 production changes with the case as H_2O_2 is detected after 30 min in case 1, after 15 min in case 2 and from 5 min in case 3. Once H_2O_2 is detected, its concentration increases almost linearly with time. The global production rate has

been estimated for each case and reported in Table 1. Values from about 10^{-3} g/h (case 1) to 10^{-2} g/h (case 3) were obtained, and are about one order of magnitude lower than those reported in [16]. This difference may be due to the lower energy used in this work, as detailed below.

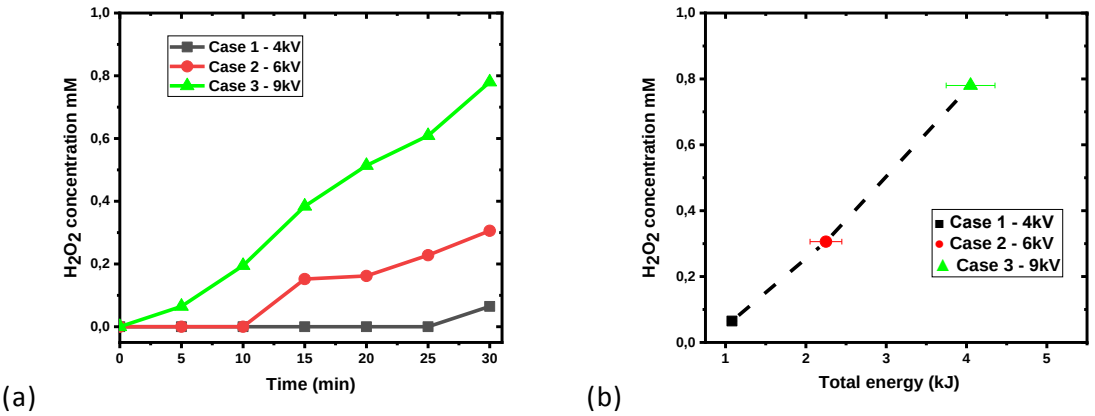

Fig. 3 Hydrogen peroxide concentration for three different cases (applied voltages). (a) Concentration of H_2O_2 as a function of time. (b) Final concentration of H_2O_2 as a function of total energy (measured after 30 min) (V = 200 mL, f = 50 Hz, Δt = 500 µs, 2 mm of gap, σ = 200 µS/cm). Uncertainty of $[H_2O_2]$ (2%) is not discernable.

The formation of hydrogen peroxide by pulsed corona discharge in deionized water use to be represented by the global reaction [7, 10, 15]:

$$6\ H_2O \rightarrow 2\ H_2O_2 + 4\ H_2 + O_2 \qquad (1)$$

Reaction (1) is assumed to be directly initiated by the discharge, to be zero-order (considering that the water concentration remains constant) [10] and to dominate the other reactions [7]. Measurements of $[H_2O_2]$ corresponding to case 3 show linear increase in relation to the time, which could be expressed as: $\frac{d[H_2O_2]}{dt} = k_1$, k_1 is the rate constant of reaction (1). This equation shows that reaction (1) dominates the H_2O_2 production. As a consequence, the rate constant k_1 can be estimated from the slope of the plot, being equal to about $k_1^{case3} = 4.7\times10^{-7}$ M/s. This model is not perfectly adapted to describe H_2O_2 production for case 1 and case 2 because of the presence of an ignition delay. Nevertheless, by using the same approach for case 2 (from 10 min), the estimation of the rate constant k_1^{case2} provides 2.3×10^{-7} M/s, which is 2 times lower than for case 3. The differences between the ignition delay and the estimated rate constant according to the cases suggest that the chemical

processes strongly depend on the discharge regime. The values of these rate constants are in good agreement with measurements obtained for needle-to-plate configurations [7, 9, 10, 13]. Using this configuration, the authors have reported up to $[H_2O_2]$ = 2 mM after 30 min, but these performances have been obtained using a very high energy (about 40 times higher than this work) [9]. For the same duration, Potocky *et al.* [18] have reported H_2O_2 concentrations equal to 1.8 mM in unbridged conditions (similar to case 1) and equal to 2.7 mM in bridged conditions (similar to case 2 or case 3). These values have been obtained using a needle-to-needle geometry with low energy (10 mJ/pulse) but for higher solution conductivities (at least 500 µS/cm) and higher electrode diameter (1 mm).

As reported in Fig.2(b), the energy delivered to the discharge depends on the case. Fig.3(b) presents the H_2O_2 concentration measured after 30 min of discharge according to the total energy consumed during the experiment. The highest the total energy, the highest the H_2O_2 concentration, and the relationship is quite linear with a coefficient of about 0.19 mM/kJ which can be interpreted as the H_2O_2 formation efficiency. The calculations of the corresponding energy yield for each case are reported in Table 1. We obtain energy yields from 1.5 g/kWh^{-1} (case 1) to 4,7 g/kWh^{-1} (case 3), which are close to the values reported in [16].

Considering these results, two different parameters are responsible for the increase in H_2O_2 production: the increase in the energy and the change of the discharge case. In order to discriminate the influence of these two parameters on H_2O_2 production, the effect of the frequency and the pulse width was inspected.

	Case 1	Case 2	Case 3
Production rate (g/h)	9.10^{-4}	4.10^{-3}	10^{-2}
Energy yield (g/(kWh)	1,5	3,3	4,7

Table 1.Hydrogen peroxide production rate and energy yields

3.3 Variation of the pulse frequency on the production of H_2O_2

In order to study independently the influence of both the total energy and the discharge case on H_2O_2 production, we have performed experiments by decreasing

the pulse frequency. This study focuses on only case 2 and case 3 experiments since H_2O_2 production is very low for case 1.

It is to notice that changing the frequency of the pulse has an influence on the total energy consumption, and also on the characteristics of the discharge. Indeed whereas only case 2 is observed for 6kV-50Hz and 6kV-25Hz, a mix of case 1 and case 2 appears for 6kV-5Hz (Fig.4). In order to isolate the influence of the total energy only, we have to adjust the applied voltage to ensure that only case 2 is present at 5 Hz, which is the case for U = 8kV. We note that these two experimental conditions (6kV-5Hz and 8kV-5Hz) give similar results in terms of energy and H_2O_2 production (Fig.4) since the mix of case 1 and case 2 involves mainly case 2 experiments. The same approach justifies the change of the applied voltage used to obtain only case 3 for different frequencies (*e.g.* 11kV-5Hz, 10kV-25Hz to obtain the whole discharge process is case 3) (Fig.4). This means that in order to keep the same case, the decrease of the frequency has to be compensated by increasing the applied voltage.

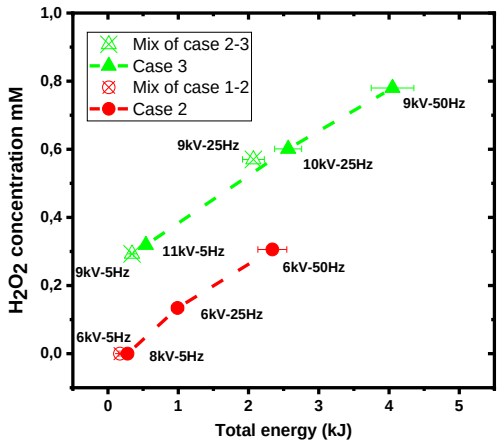

Fig. 4 H_2O_2 concentration according to the total energy for 2 different cases (V = 150 mL, Δt = 500 µs, 2 mm of gap, σ = 200 µS/cm) – couples "*applied voltage – frequency*" are reported. Uncertainty of [H_2O_2] (2%) is not discernable.

Fig.4 shows that, for a given case (either for case 2 or case 3), the increase of the energy involves the increase of [H_2O_2]. The evolution is almost linear with a coefficient equal to about 0.12 mM/kJ for both cases. This value is lower than those estimated from Fig.3(b) (0.19 mM/kJ), which includes the influence of both the total energy and the discharge case. It confirms that both parameters exercise comparable influence on H_2O_2 production. This result is also observable directly on Fig.4 which

shows that for a same total energy, the concentration of H_2O_2 in case 3 is greater than that in case 2. For example at 2.5 kJ, case 3 conditions (10kV-25Hz) produce twice more H_2O_2 than case 2 conditions (6kV-50Hz). These results are in good agreement with the rate constants estimated previously which have shown that k_1^{case2} is 2 times lower than k_1^{case3}. These results confirm that chemical processes involved in the discharge mechanisms strongly depend on the discharge regime (case). They are consistent with [16], which suggests that the power is not the only parameter determining H_2O_2 production.

3.4 Effect of pulse duration on the production of H_2O_2

In order to analyze the effect of the discharge regime on the H_2O_2 production, the length of the pulse duration is changed from 50 to 500 µs. Fig. 5 presents the results obtained for case 2 (6 kV) and case 3 (9 kV). We observe that increasing the pulse duration from 50 to 500 µs involves a low increase of the deposited energy equal to 25% for case 2 (from 1.8 kJ to 2.25 kJ) and to 12% for case 3 (from 3.7 kJ to 4.1 kJ). Indeed, as mentioned previously (Fig. 2(b)), most part of the energy is deposited before 50 µs (before the first breakdown).

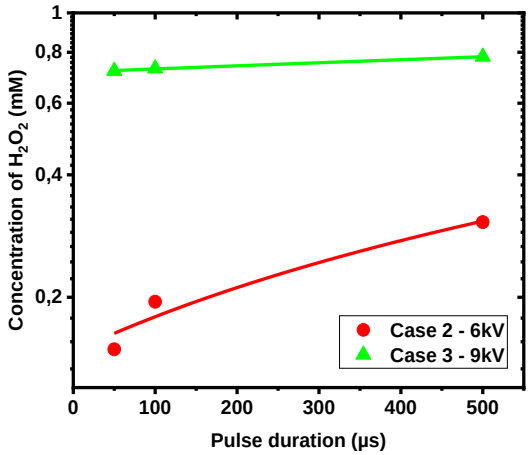

Fig. 5 H_2O_2 production measured for different pulse durations (Δt =50,100,500 µs) and reported for 2 different cases (V = 200 mL, f = 50 Hz, 2 mm of gap, σ= 200 µS/cm). Uncertainty of [H_2O_2] (2%) is not discernable

Whereas the variation of the energy is similar for both cases, the influence of the pulse duration is different on H_2O_2 production. From 50 to 500 µs, the concentration of H_2O_2 increases by 100% for case 2 (from 0.15 to 0.3 mM), but by only 10% for

case 3 (from 0.72 to 0.78 mM) (Fig.5). This result shows that the chemical kinetics initiated by the discharge was very different for case 2 and case 3. Experiments at 50 µs give information on what happens during the pre-breakdown and the breakdown: the chemical mechanisms are much more efficient for case 3 than for case 2 for these stages. To increase the pulse duration from 50 µs to 500 µs means increasing the post-breakdown duration. During this phase H_2O_2 production is much more efficient for case 2 than for case 3. H_2O_2 production seems to be mainly driven by the initial stage of the discharge in case 3 whereas the tail of the discharge has also a significant influence for case 2. These results confirm that the chemical processes induced by the discharge are very different according to the regime.

3.5 Effect of different electrode materials on H_2O_2 formation

We have shown that case 3 is more efficient than case 2 for H_2O_2 production. Even if energy cost and chemical efficiency are important parameters of the process, its durability is also essential. The weak point of such process is the lifetime of the electrodes. According to the physical and chemical mechanisms occurring during the discharge, and to the nature of electrode material, the erosion phenomena are very different [21]. Before studying the erosion processes, we propose to investigate for our experimental conditions the influence of the electrodes material on the H_2O_2 production.

Fig. 6 shows H_2O_2 concentration obtained using electrodes in tungsten (dotted curve), platinum (solid curve) and a combination of platinum for the anode and tungsten for the cathode (dash and dot curve). The measurements have been performed for 3 different applied voltages and during 30 min of discharge, except for experiments using platinum electrodes at 6 kV and 9 kV (solid curve) because of the total erosion of the cathode (GND) after 10 min.

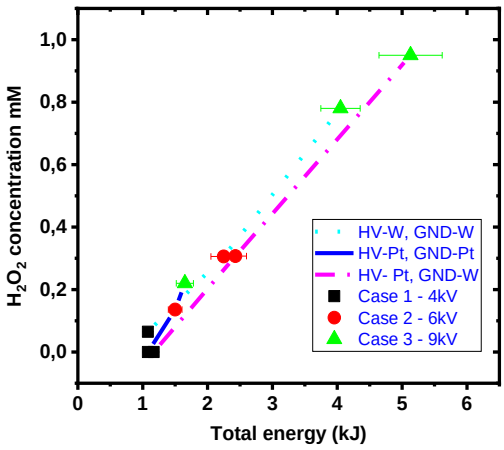

Fig. 6. The effect of electrode material on the production of H_2O_2 by the discharge in water (V = 200 mL, f = 50 Hz, Δt = 500 µs, 2 mm of gap, σ = 200 µS/cm). HV means anode and GND is for cathode. Uncertainty on $[H_2O_2]$ is not discernable (2%)

For case 1 and case 2, the electrode material has no influence on the total energy consumed after 30 min of discharge, as already observed by [13]. For case 3 we observe that the total energy consumed during the experiment is about 20% higher for Pt-W electrodes than for W-W electrodes (using the same applied voltage).

On the whole range of energy, the influence of the electrode material on the H_2O_2 production is low. At very low energy (1.08 kJ), H_2O_2 is not detected either with Pt-electrodes or with Pt-W electrodes, whereas a low concentration is measured with W-electrodes ($[H_2O_2]$ = 0.065 mM). For medium energy (~2 kJ), the concentrations of H_2O_2 are similar whatever the electrode material (~0.25 mM). Finally at high energy (4-5 kJ) the concentration of H_2O_2 generated after using the combination of two different materials for the electrodes is similar to the production obtained with W-electrodes (for a given energy).

This result is consistent with [13, 18], which have reported no influence of the electrode material on the initial H_2O_2 formation rates. However, it has been shown that after several tens of minutes of discharge, tungsten particles dissolved into the bulk solution via the electrodes erosion, lead to H_2O_2 decomposition by catalysis reactions [11, 13]. Moreover, it has been shown that hydrogen peroxide concentration can be affected when Pt is used (depending on the pH) [19]. Therefore, in addition to limiting the process, the erosion of electrodes by electrical discharge in water can modify the chemical activity in the solution. Even if such catalytic effect

has not been observed in our conditions, the erosion of tungsten and platinum electrodes is investigated in detail in the next section.

4. Erosion of electrodes

The erosion of the electrodes is estimated from the decrease of the length of the protruding part with time. In situ measurements have been performed every 5 min using an IDS camera. Even though the measurements have shown that the erosion is all around the electrodes, the variation of the length is a good indicator to describe the erosion process. Fig.7 shows the time evolution of the normalized length of positive (HV) and ground (GND) electrodes for experiments performed with either W or Pt at 3 different applied voltage (*i.e.* different energies per pulse which involve different cases).

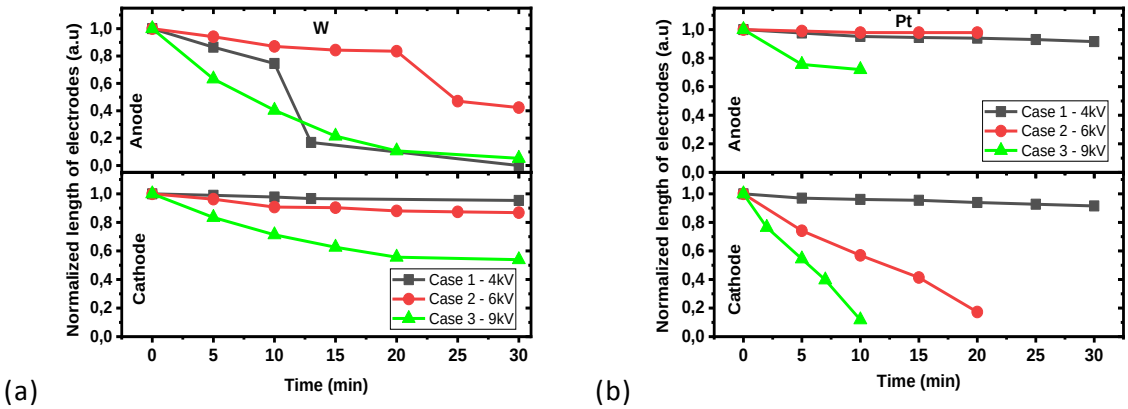

Fig. 7 Variation of normalized length of anode and cathode electrodes as a function of time, (a) tungsten electrodes, (b) platinum electrodes (V = 150 mL, f = 50 Hz, Δt = 500 µs, 2 mm of gap, σ = 200 µS/cm). Uncertainty of measurement is not discernable (2%)

It is obvious that the erosion of both materials (tungsten and platinum) increases with the discharge time. However, the erosion of electrodes strongly depends on the material, the case and the energy per discharge.

It is to notice that for case 1 (*e.g.* discharge in cathode regime without breakdown), the erosion of both electrodes is not significant for both materials (decrease lower than 10%), except for W-anode which shows a fast decrease (85%) after 10 min of discharge. The variation of the electrodes length for case 2 (*e.g.* discharge in cathode regime with breakdown) is significant for W-anode (55%) and Pt-cathode (85%) but negligible for W-cathode (15%) and Pt-anode (5%). This work does not highlight the

influence of the breakdown phenomena on the erosion process for cathode regime neither on W or Pt electrodes, whereas Potocký *et al.* have shown that the erosion rate for an unbridged discharge was lower than for a bridged discharge with W electrodes [18].

Nevertheless, when dealing with electrodes discharge-induced erosion, several processes might be considered, as presented in other works [19, 20, 22]. One of these processes concerns electrochemical reactions that may occur at the electrodes surface. In the case of tungsten electrodes, the anodic oxidation of W to WO_3 [33], followed by the oxide dissolution into tungstate ions, WO_4^{2-} [29], is to be considered:

$$W + 3H_2O \rightarrow WO_3 + 6H^+ + 4e^- \quad (2)$$

$$WO_3 + H_2O \rightarrow WO_4^{2-} + 2H^+ \quad (3)$$

This mechanism could explain the W-anode length decrease presented in Fig.7(a) whereas no significant change is observed for the cathode.

For the platinum electrodes, a significant length variation is only observed at the cathode. Once again, we might take into account the possible cathodic reactions taking place during the process, one of these being oxygen reduction:

$$O_2 + 2H_2O + 4e^- \rightarrow 4OH^- \quad (4)$$

In addition, the presence of chloride ions might have a role in the erosion of Pt electrodes [34] according to the reactions:

$$Pt + 4Cl^- \rightarrow [PtCl_4]^{2-} + 2e^- \quad (5)$$

$$Pt + 6Cl^- \rightarrow [PtCl_6]^{2-} + 4e^- \quad (6)$$

Thus, cathodic reduction of oxygen added to an easier oxidation of Pt electrodes in the presence of chloride ions could explain the significant length change observed at the Pt-cathode.

Regarding breakdown conditions, the erosion of both electrodes is always more important for case 3 (initiation of the discharge from the anode) than for case 2 (from the cathode), which is expected since the energy per pulse is higher in case 3 than in

case 2 (Fig.2(a)). Furthermore, for W electrodes (Fig.7(a)), erosion is more important at the anode than at the cathode, showing respective variations of 55%/15% for case 2 and 90%/45% for case 3. This result is consistent with experiments performed in plate-plate configuration [22]. Liu *et al.* suggested that a larger amount of mass is lost from the anode since the arc develops from the anode. This phenomenon can only explain case 3 results since for case 2 the discharge is initiated from the cathode.

In contrast, for platinum electrodes (Fig.7(b)) erosion is less intense at the anode than at the cathode, showing respective variations of 5%/85% for case 2 and 30%/90% for case 3. These results justify experiments performed with a combination of material using platinum for the anode and tungsten for the cathode. This configuration gives the best result in terms of electrodes erosion. We point out that the evolution of the electrodes showed similar behavior to Fig.7(a) for cathode and Fig.7(b) for anode (not shown here).

The decreases in the length are almost linear for all the conditions presented in Fig.7, except for the tungsten anode electrode in case 1 (as already reported), and in case 2, for which a fast decrease occurs after 20 min of discharge. These results will be discussed below.

The morphology of the electrodes exposed to the discharge is studied with electronic microscopy. Fig. 8 shows SEM images of anode and cathode for W and Pt electrodes after plasma discharge in water. Complementary SEM images (pin orientation and higher magnification) are provided in supplementary material 1. These images confirm the results shown in Fig.7. The initial shapes of the electrodes are sharp and they became rounded after discharge exposure, except for HV-Pt, GND-W and more slightly for GND-Pt used in case 1 (Fig.8(a)); as well as for HV-Pt and GND-W used in case 2 (Fig.8(b)), conditions for which the erosion process is not significant.

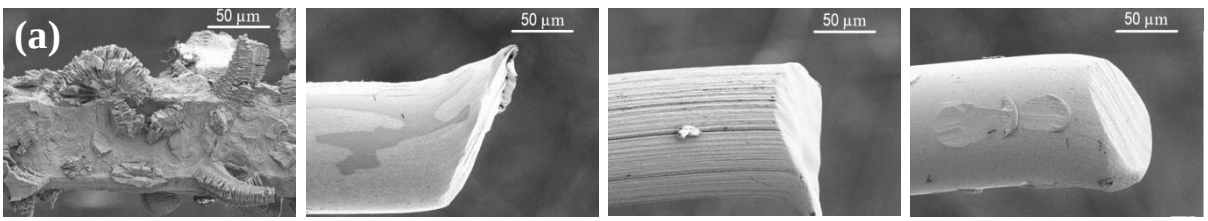

HV - W 4kV – after 10min	HV - Pt 4kV – after 15min	GND - W 4kV – after 10min	GND - Pt 4kV – after 15min

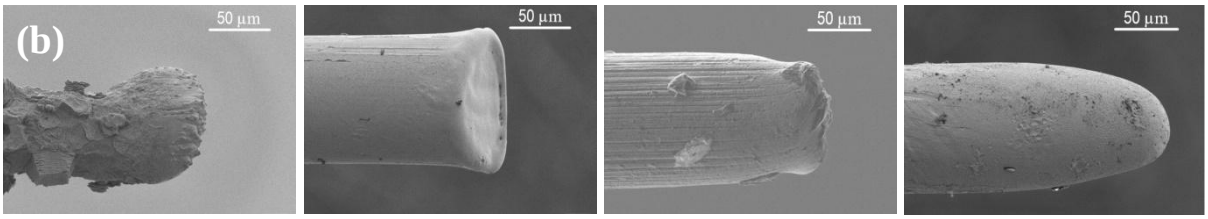

HV - W 6kV – after 15min	HV - Pt 6kV – after 10min	GND - W 6kV – after 15min	GND - Pt 6kV – after 10min

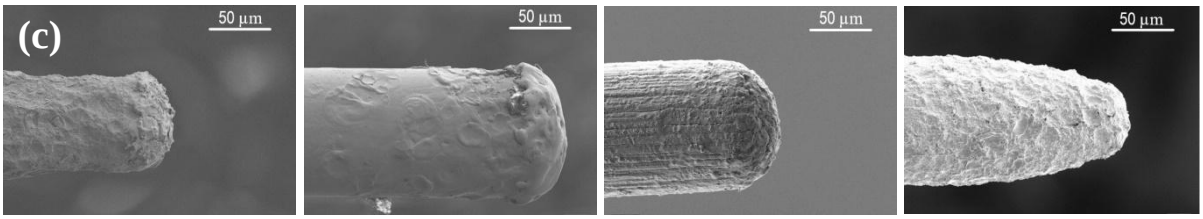

HV - W 9kV – after 15min	HV - Pt 9kV – after 5min	GND - W 9kV – after 15min	GND - Pt 9kV – after 5min

Fig. 8 SEM images of the eroded tip of tungsten and platinum electrodes after the electrical discharge obtained for (a) case 1 (4kV), (b) case 2 (6 kV) and (c) case 3 (9kV), anode and cathode are shown on left and right respectively (V = 150 mL, f = 50Hz, Δt = 500µs, 2mm of gap, and σ = 200 µS/cm) with a ×500 magnification

The results show the diversity of the surface states according to the polarity and the materials, which confirms that many physical and chemical processes take action on electrodes erosion during pulse discharges in water [20-22].

We remind that case 1 corresponds to cathode initiation of the discharge which does not span the electrodes gap. Based on previous studies [18, 20, 22], we can state that for case 1, the dominant process that causes the electrode erosion is electrochemistry involving anodic electrodissolution (anodic oxidation + electrolyte dissolution). Indeed, the erosion process is only significant for HV-W electrode, which presents a lower standard potential than platinum. This result is also confirmed by EDX measurements which reports almost 17% of oxygen on the HV-W surface whereas no [O] trace is detected for other electrodes. It has been suggested that electrolysis is

most predominant before the formation of the conductive channel in the water but when electrons arrive to the anode, they inhibit the anodic electrodissolution [20].

As a consequence, we observe that for case 2 (cathode initiation with breakdown), the body of HV-W also shows typical patterns for electrochemical oxidation process, *i.e.* the surface is not smooth anymore whereas the tip of the electrode, which receives a high electron bombardment through the conductive channel, shows mainly protrusions. On the contrary, the HV-Pt electrode presents a smooth surface. Thermal processes are primarily responsible for the erosion which is due to melting (evaporation can also be considered) followed by condensation. The differences observed on the surface roughness can be explained by the physical properties of tungsten and platinum. Tungsten has much higher thermal conductivity than platinum which leads to a faster solidification of the tungsten surface after melting. As a result, the molten tungsten part quickly solidifies to produce a thorny structure on the tip of electrode surface, while a slower solidification of platinum leads the smoother electrode surface [11, 13, 20]. Both ground electrodes also show patterns characteristic to thermal processes but we also report spherical cavities that can be due to ions bombardment.

For case 3, the energy per pulse is higher so the electrochemical and bombardment processes are no more significant in comparison to thermal effect. Surface patterns of the electrodes are quite similar to those observed for case 2, except for GND-Pt which shows smooth crater like surface with no more cavities.

It is to notice that cracks have been observed on W-electrodes which can be explained by the fact that at high temperatures, tungsten recrystallizes and becomes brittle [35], whereas platinum is known to be fragile. This property can explain the break of the electrode tip reported for HV-W in case 1 and case 2 after 10 and 20 minutes of discharge, respectively.

5. Conclusion

We studied the formation of hydrogen peroxide in water by pin-to-pin micro-pulsed discharge and the resulting electrodes erosion. We have estimated concentrations of H_2O_2 for the three different discharge modes of operation: case 1 (cathode regime –

no breakdown), case 2 (cathode regime – breakdown) and case 3 (anode regime – breakdowns). Besides different mechanisms, the cases also consume different total energies (estimated over 30 min of process): case 1 - 1.1 kJ, case 2 - 2.2 kJ and case 3 - 4.1 kJ. We report that the concentration of H_2O_2 changes with both the cases and the energy, the influence of these two parameters being in the same order of magnitude. On the one hand, we have reported that the hydrogen peroxide concentration increases linearly with the total energy. On the other hand, we have shown that, for a given energy, case 3 produces more H_2O_2 than case 2. The highest concentration of H_2O_2 is formed for discharges propagating from the anode. Moreover, we have highlighted that the post discharge plays an important role in case 2, whereas it does not affect significantly the concentration of H_2O_2 in case 3. These results confirm that the two discharge regimes (cathode and anode) involve very different initiation and propagation mechanisms, which result in different chemical mechanisms.

Finally, we have demonstrated that the production of H_2O_2 does not depend on the electrode materials by comparing tungsten and platinum. Regarding the strong erosion occurring during the process, we have performed experiments with a combination using W-cathode and Pt-anode that allows improving the process lifetime. Time evolution of the electrodes' length and SEM images provide new and complementary results in order to study the erosion processes according to the discharge cases, the material and the polarity of the electrodes. We suggest that for case 1, the dominant process of electrode erosion is electrochemistry (anodic oxidation followed by electrolyte dissolution) which is only significant at the anode. For case 2 and case 3, this process is no more significant but thermal processes are dominant in the erosion process.

This work contributes to a better understanding of pin-to-pin micro-pulsed discharges in water. H_2O_2 measurements together with the erosion study highlight very different mechanisms involved in the discharge according to the case. Studying H_2O_2 concentration is the first step to study the complex chemical activities in the solution after plasma discharge. Chemical components are thought to have many applications in wastewater treatment, medicine, and biology.

Acknowledgment

This work bearing the reference ANR-11-LABX-086 has benefited from State aid managed by the National Research Agency under the Future Investments program with the reference number ANR-18-IDEX- 0001

The authors would like to thank the technical support in LSPM and LPL for providing the SEM, EDX and UV-Vis analyses.

6. References

1. Akiyama, H., *Streamer discharges in liquids and their applications.* IEEE Transactions on Dielectrics and Electrical Insulation, 2000. **7**(5): p. 646-653.
2. Bruggeman, P. and C. Leys, *Non-thermal plasmas in and in contact with liquids.* Journal of Physics D: Applied Physics, 2009. **42**(5): p. 053001.
3. Locke, B., et al., *Electrohydraulic discharge and nonthermal plasma for water treatment.* Industrial & Engineering Chemistry Research, 2006. **45**(3): p. 882-905.
4. Locke, B.R., *Special Issue on Plasmas and Liquids.* Plasma Processes and Polymers, 2009. **6**(11): p. 711-712.
5. Šunka, P., *Pulse electrical discharges in water and their applications.* Physics of Plasmas, 2001. **8**(5): p. 2587-2594.
6. Lukes, P., et al. *Role of solution conductivity in the electron impact dissociation of H2O induced by plasma processes in the pulsed corona discharge in water*. in *Proceedings, 19th International Symposium on Plasma Chemistry*. 2009.
7. Kirkpatrick, M.J. and B.R. Locke, *Hydrogen, oxygen, and hydrogen peroxide formation in aqueous phase pulsed corona electrical discharge.* Industrial & Engineering Chemistry Research, 2005. **44**(12): p. 4243-4248.
8. Malik, M.A., A. Ghaffar, and S.A. Malik, *Water purification by electrical discharges.* Plasma Sources Science and Technology, 2001. **10**(1): p. 82-91.
9. Grymonpré, D.R., et al., *Hybrid gas− liquid electrical discharge reactors for organic compound degradation.* Industrial & Engineering Chemistry Research, 2004. **43**(9): p. 1975-1989.
10. Joshi, A.A., et al., *Formation of hydroxyl radicals, hydrogen peroxide and aqueous electrons by pulsed streamer corona discharge in aqueous solution.* Journal of Hazardous Materials, 1995. **41**(1): p. 3-30.
11. Lukes, P., et al., *The catalytic role of tungsten electrode material in the plasmachemical activity of a pulsed corona discharge in water.* Plasma Sources Science and Technology, 2011. **20**(3): p. 034011.
12. Lukes, P., A.T. Appleton, and B.R. Locke, *Hydrogen peroxide and ozone formation in hybrid gas-liquid electrical discharge reactors.* IEEE Transactions on Industry Applications, 2004. **40**(1): p. 60-67.
13. Holzer, F. and B.R. Locke, *Influence of High Voltage Needle Electrode Material on Hydrogen Peroxide Formation and Electrode Erosion in a Hybrid Gas–Liquid Series Electrical Discharge Reactor.* Plasma Chemistry and Plasma Processing, 2008. **28**(1): p. 1-13.
14. Sahni, M. and B.R. Locke, *Quantification of Hydroxyl Radicals Produced in Aqueous Phase Pulsed Electrical Discharge Reactors.* Industrial & Engineering Chemistry Research, 2006. **45**(17): p. 5819-5825.

15. Medodovic, S. and B.R. Locke, *Primary chemical reactions in pulsed electrical discharge channels in water.* Journal of Physics D: Applied Physics, 2009. **42**(4): p. 049801-049801.
16. Locke, B.R. and K.-Y. Shih, *Review of the methods to form hydrogen peroxide in electrical discharge plasma with liquid water.* Plasma Sources Science and Technology, 2011. **20**(3): p. 034006.
17. Locke, B.R. and S.M. Thagard, *Analysis and review of chemical reactions and transport processes in pulsed electrical discharge plasma formed directly in liquid water.* Plasma Chemistry and Plasma Processing, 2012. **32**(5): p. 875-917.
18. Potocký, Š., N. Saito, and O. Takai, *Needle electrode erosion in water plasma discharge.* Thin Solid Films, 2009. **518**(3): p. 918-923.
19. Međedović, S. and B.R. Locke, *Platinum catalysed decomposition of hydrogen peroxide in aqueous-phase pulsed corona electrical discharge.* Applied Catalysis B: Environmental, 2006. **67**(3-4): p. 149-159.
20. Lukeš, P., et al., *Erosion of needle electrodes in pulsed corona discharge in water.* Czechoslovak Journal of Physics, 2006. **56**(2): p. B916-B924.
21. Goryachev, V., A. Ufimtsev, and A. Khodakovskii, *Mechanism of electrode erosion in pulsed discharges in water with a pulse energy of ~ 1 J.* Technical Physics Letters, 1997. **23**(5): p. 386-387.
22. Liu, Y., et al., *Comparison and Evaluation of Electrode Erosion Under High-Pulsed Current Discharges in Air and Water Mediums.* IEEE Transactions on Plasma Science, 2016. **44**(7): p. 1169-1177.
23. Kirkpatrick, M.J. and B.R. Locke, *Effects of Platinum Electrode on Hydrogen, Oxygen, and Hydrogen Peroxide Formation in Aqueous Phase Pulsed Corona Electrical Discharge.* Industrial & Engineering Chemistry Research, 2006. **45**(6): p. 2138-2142.
24. Patel, M.R., et al., *Theoretical models of the electrical discharge machining process. II. The anode erosion model.* Journal of applied physics, 1989. **66**(9): p. 4104-4111.
25. DiBitonto, D.D., et al., *Theoretical models of the electrical discharge machining process. I. A simple cathode erosion model.* Journal of applied physics, 1989. **66**(9): p. 4095-4103.
26. Xu, Z.Y., et al., *An electrochemical discharge drilling method of small deep holes.* The International Journal of Advanced Manufacturing Technology, 2018. **95**(5-8): p. 3037-3044.
27. Yerokhin, A.L., et al., *Plasma electrolysis for surface engineering.* Surface and Coatings Technology, 1999. **122**(2–3): p. 73-93.
28. Kumar, P.D., et al., *Erosion and lifetime evaluation of molybdenum electrode under high energy impulse current.* IEEE Transactions on Plasma Science, 2011. **39**(4): p. 1180-1186.
29. Anik, M. and K. Osseo-Asare, *Effect of pH on the Anodic Behavior of Tungsten.* Journal of The Electrochemical Society, 2002. **149**(6): p. B224-B233.
30. Rond, C., et al., *Time-resolved diagnostics of a pin-to-pin pulsed discharge in water: pre-breakdown and breakdown analysis.* Journal of Physics D: Applied Physics, 2018. **51**(33): p. 335201.
31. Eisenberg, G., *Colorimetric determination of hydrogen peroxide.* Industrial & Engineering Chemistry Analytical Edition, 1943. **15**(5): p. 327-328.
32. Rond, C., et al., *Influence of applied voltage and electrical conductivity on underwater pin-to-pin pulsed discharge.* Journal of Physics D: Applied Physics, 2018. **52**(2): p. 025202.
33. DEPETRIS-WERY, M. and J.-C. CATONNÉ, *Potentiels standards d'oxydo-réduction en solution aqueuse-Application aux traitements de surface en voie humide.* 2014.

34. Matsuoka, K., et al., *Degradation of polymer electrolyte fuel cells under the existence of anion species.* Journal of Power Sources, 2008. **179**(2): p. 560-565.
35. Ceccato, P., *Filamentary plasma discharge inside water: initiation and propagation of a plasma in a dense medium*, 2009, Ecole Polytechnique X.